Natural Science Report, Ochanomizu University, Vol. 41, No. 1, 1990
お茶の水女子大学 自然科学報告 第41巻 第1号

# Analysis of the $\pi$-Electronic Structure of Infinitely Large Networks

**Ying-Duo Gao and Haruo Hosoya**

Department of Chemistry, Ochanomizu University,
Bunkyo-ku, Tokyo 112, Japan

## Abstract

In order to expand the Coulson and Longuet-Higgins' integral method to infinitely large conjugated $\pi$-electronic networks, such as branched polyenes and periodic polyacenes, two new efficient techniques are proposed. The analytical solutions of bond orders and $\pi$-electronic energy of these two kinds of networks with various modes of bond alternation are derived, which are expressd in terms of the three kinds of the elliptic integrals. The benzene characters for polycyclic aromatics are also obtained. The dependency of these results on the bond alternation parameter can explicitly be discussed.

## I. Introduction

Although calculations of the Hückel molecular orbitals for various series of hydrocarbon molecules have been studied by many people [1-21], the analytical solutions of $\pi$-electronic energy and bond orders with bond alternation were rarely obtained, especially for infinitely large networks. The Coulson's integral method for deriving the analytical solutions of the $\pi$-electronic energy and bond orders are found to be powerful for fairly large molecules. However, for infinitely large polymers, this method cannot be used directly.

One of the present authors proposed two counting polynomials [22] to enable the calculation for infinitely large polyenes by the use of their recursive relations [23]. Further, the method for applying the Coulson's integral to infinitely large periodic networks is also found, and has been used for infinitely large polyacene and polyphenanthrene successfully [24].

In this paper, we give a brief account of our methods for the calculations of several series of infinitely large networks, and summarize their analytical solutions. Several new results are also given.

In the following discussion, we will be concerned with the case in which bond alternation is explicitly taken into consideration. For the simplest case the bonds are grouped into single ($s$) and double ($d$) bonds. The bond alternation parameter $a$ is defined as the ratio of the resonance integral of an $s$ bond ($\beta_s$) to that of a $d$ bond ($\beta_d$) in the HMO scheme, namely $a=\beta_s/\beta_d$, with $0 \leqq a \leqq 1$.

## II. Coulson's Integral Method

The total $\pi$-electronic energy $E_\pi$ of the closed shell ground state of an unsaturated molecule $G$ with $N$-electrons can be expressed as

$$\begin{aligned} E_\pi &= 2\sum_{n=1}^{[N/2]} x_n \\ &= \frac{1}{i\pi}\oint_\gamma \left[\frac{z\Delta'_G(z)}{P_G(z)} - N\right] dz \\ &= \frac{1}{\pi}\int_{-\infty}^{\infty} \left[\frac{iz\Delta'_G(iz)}{P_G(iz)} - N\right] dz, \end{aligned} \qquad (1)$$

where $\gamma$ is the infinitely large semicircle in the complex plane. $P_G(x)$ is the characteristic polynomial of $G$, also denoted as $\Delta_G(x)$,

$$P_G(x) = \Delta_G(x) = \sum_{k=0}^{N} a_k x^{N-k}, \qquad (2)$$

and $\Delta'_G(x)$ is the first derivative of $\Delta_G(x)$.

The Coulson's bond order of bond $l$ in $G$ is expressed as

$$\begin{aligned} p_l &= -\frac{1}{i\pi}\oint_\gamma \frac{\Delta_{rs}(z)}{P_G(z)} dz \\ &= (-1)^{r+s+1}\frac{1}{\pi}\int_{-\infty}^{\infty} \frac{\Delta_{rs}(ix)}{P_G(ix)} dx, \quad (l=\overline{rs}) \end{aligned} \qquad (3)$$

where $\Delta_{rs}(x)$ is the subdeterminant obtained by deleting the $r$-th row and $s$-th column from $\Delta_G(x)$.

Equations (1) and (3) can directly be applied to small molecules. However, for infinitely large networks, the first problem we encounter is that the integrands of (1) and (3) cannot easily be expressed. Here, we propose two approaches for extending the Coulson's integral method to infinitely large branched polymers and periodic networks, respectively.

## III. Calculation of the Infinitely Large Polyenes

For the calculation of the infinitely large branched polyenes, the key point is to break down the large structure into several smaller parts, in other words, to express the integrands of Eqs. (1) and (3) in terms of the recursive relations involving the step-up operators $\alpha$ and $\beta$.

Two polynomials $f_G(x)$ and $q_G(x)$ are defined as follows [22],

$$q_G(x)=\sum_{k=0}^{[N/2]}(-1)^k a_{2k}x^k\,, \tag{4}$$

$$f_G(x)=\sum_{k=0}^{[N/2]}(-1)^k a_{2k}x^{N-2k}\,, \tag{5}$$

in which, $a_{2k}$ are the coefficients of $P_G(x)$ in Eq. (2).

These polynomials are related with each other as

$$q_G(x)=(\sqrt{x}/i)^N P_G(i/\sqrt{x})\,, \tag{6}$$

and

$$f_G(x)=(1/i)^N P_G(ix)\,. \tag{7}$$

Two sets of the recursion formulas of $q_G(x)$ and $f_G(x)$ are written down as follows, depending on the choice of the pivot bond as $s$ (single) or $d$ (double),

$$q_G(x)=q_{G-s}(x)+a^2xq_{G\ominus s}(x)\,, \tag{8}$$

$$q_G(x)=q_{G-d}(x)+xq_{G\ominus d}(x)\,, \tag{9}$$

$$f_G(x)=f_{G-s}(x)+a^2f_{G\ominus s}(x)\,, \tag{10}$$

$$f_G(x)=f_{G-d}(x)+f_{G\ominus d}(x)\,. \tag{11}$$

Then the $\pi$-electronic energy $E_\pi$ and the bond order can be expressed as

$$E_\pi=\frac{4}{\pi}\int_0^\infty\frac{q_G'(x^2)}{q_G(x^2)}dx\,, \tag{12}$$

$$\begin{aligned}p_l&=\frac{2}{\pi}\int_0^\infty\frac{q_{G\ominus l}(x^2)}{q_G(x^2)}dx\\&=\frac{2}{\pi}\int_0^\infty\frac{f_{G\ominus l}(x)}{f_G(x)}dx\,.\end{aligned} \tag{13}$$

Further, we define the step-up operators $\alpha_{2n}^f(x)$, $\beta_{2n+1}^f(x)$ for the polynomial $f_G(x)$ as

$$\alpha_{2n}^f(x)=\frac{f_{2n}(x)}{f_{2n-1}(x)}=x+\frac{1}{\beta_{2n-1}^f(x)}\,, \tag{14}$$

$$\beta_{2n+1}^f(x)=\frac{f_{2n+1}(x)}{f_{2n}(x)}=x+\frac{a^2}{\alpha_{2n}^f(x)}\,. \tag{15}$$

For infinitely large networks, $\alpha_{2n}^f(x)$, $\beta_{2n+1}^f(x)$ are expected to converge to certain limits, which are solved, respectively, to be

$$\alpha^f_{2n}(x)\to\alpha^f(x)=\frac{x^2+(1-a^2)+\sqrt{x^4+2(1+a^2)x^2+(1-a^2)^2}}{2x}, \qquad (16)$$

and

$$\beta^f_{2n+1}(x)\to\beta^f(x)=\frac{x^2-(1-a^2)+\sqrt{x^4+2(1+a^2)x^2+(1-a^2)^2}}{2x}. \qquad (17)$$

Then the integrands of Eqs. (1) and (3) for infinitely large polyenes can be obtained easily.

Consider polyacetylene as shown in Chart 1, with $2n$ carbon atoms, and see how it behaves when $n$ tends to infinity. In order to calculate the bond order of the terminal bond 1, 2, we get

$$f_G(x)=f_{2n}(x), \qquad (18)$$

$$f_{G\ominus l}(x)=f_{2n-2}(x). \qquad (19)$$

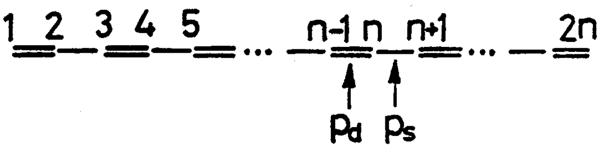

Chart 1.

According to Eq. (13), we have

$$p_{12}=\frac{2}{\pi}\int_0^\infty\frac{f_{2n-2}(x)}{f_{2n}(x)}dx. \qquad (20)$$

By using the step-up operators, Eq. (20) can be expressed as

$$p_{12}=\frac{2}{\pi}\int_0^\infty\frac{1}{\alpha(x)\beta(x)}dx. \qquad (21)$$

By substituting Eqs. (16) and (17) into (21), the analytical expression of $p_{12}$ is obtained as

$$p_{12}(a)=\frac{4}{3\pi a^2}[(a^2+1)E(a)-(1-a^2)K(a)], \qquad (22)$$

where $K$ and $E$ are the first and second kind complete elliptic integrals, respectively [26],

$$K(k)=\int_0^{\pi/2}\frac{d\theta}{\sqrt{1-k^2\sin^2\theta}}, \qquad (23)$$

$$E(k)=\int_0^{\pi/2}\sqrt{1-k^2\sin^2\theta}\,d\theta. \qquad (24)$$

Similarly, $p_{23}$, $p_{34}$ and $p_{45}$ are derived as

$$p_{23}=\frac{2}{\pi}\int_0^{\infty}\frac{af_1(x)f_{2n-3}(x)}{f_{2n}(x)}dx=\frac{2a}{\pi}\int_0^{\infty}\frac{x}{\alpha^2(x)\beta(x)}dx\,, \tag{25}$$

$$p_{34}=\frac{2}{\pi}\int_0^{\infty}\frac{f_2(x)f_{2n-4}(x)}{f_{2n}(x)}dx=\frac{2}{\pi}\int_0^{\infty}\frac{x^2+1}{[\alpha(x)\beta(x)]^2}dx\,, \tag{26}$$

and

$$p_{45}=\frac{2a}{\pi}\int_0^{\infty}\frac{f_3(x)f_{2n-5}(x)}{f_{2n}(x)}dx=\frac{2a}{\pi}\int_0^{\infty}\frac{x(x^2+2)}{[\alpha(x)]^3[\beta(x)]^2}dx\,. \tag{27}$$

Finally, they can be expressed as,

$$p_{23}(a)=\frac{4}{15\pi a^3}[(a^4+9a^2-4)E(a)-(7a^2-4)(1-a^2)K(a)]\,, \tag{28}$$

$$\begin{aligned}p_{34}(a)=\frac{8}{105\pi a^4}[&2(-a^6+12a^4-2a^2+6)E(a)\\&-(a^4+2a^2+12)(1-a^2)K(a)]\,,\end{aligned} \tag{29}$$

and

$$\begin{aligned}p_{45}(a)=\frac{8}{315\pi a^5}[&2(2a^8+2a^6+42a^4+5a^2-16)E(a)\\&+(2a^6-75a^4+6a^2+32)(1-a^2)K(a)]\,.\end{aligned} \tag{30}$$

The bond orders of other bonds, such as bonds 5,6 and 6,7 can also be obtained with the same approach. However, the closer the bond is to the center of the infinitely long chain, the more complicated the calculation is.

The bond orders $p_{12}$, $p_{23}$, $p_{34}$ and $p_{45}$ are plotted against the bond alternation parameter $a$ as shown in Fig. 1, where the curves of the central bond orders $p_s$ and $p_d$ are also plotted. Although $p_s$ and $p_d$ can be obtained by the same method, the calculations become easier by using the method

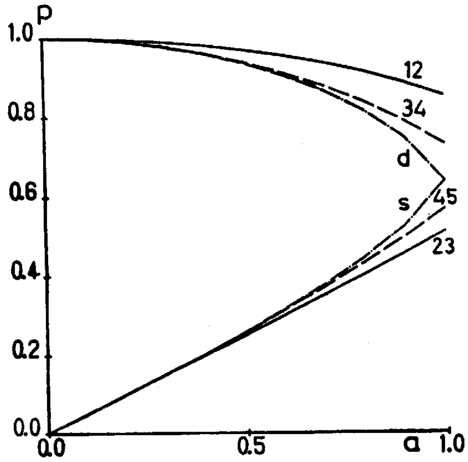

Fig. 1. The curves of the bond orders of the terminal bonds for polyacetylene as a function of the bond alternation parameter $a$. The —·—· lines are those of the central bonds.

for the periodic networks. In the next section, we will give the derivations in detail.

Next, let us consider infinitely large branched polyene $Y$ as shown in Chart 2(a). It is composed of one polyacetylene of length $2k+1$ and two identical polyacetylenes of length $2k$. The $f_G$ polynomial of $Y$ can be derived by cutting $d1$ in Chart 2(a), and we get

$$\begin{aligned} f_G(x) &= f_{4k+1}(x) f_{2k+1}(x) + f_{2k}^3(x) \\ &= f_{2k}(x)[f_{2k+1}^2(x) + a^2 f_{2k-1}(x) f_{2k+1}(x)] + f_{2k}^3(x) . \end{aligned} \tag{31}$$

For the central double bond $p_{d1}$,

$$f_{G\ominus d1}(x) = f_{2k}^3(x) . \tag{32}$$

Then, according to Eqs. (11), (14) and (15), we have

$$\begin{aligned} p_{d1} &= \frac{2}{\pi} \int_0^\infty \frac{f_{2k}^3(x)}{f_{2k}(x)[f_{2k+1}^2(x) + a^2 f_{2k-1}(x) f_{2k+1}(x)] + f_{2k}^3(x)} dx \\ &= \frac{2}{\pi} \int_0^\infty \frac{1}{\beta^2(x) + a^2 \beta(x)/\alpha(x) + 1} dx . \end{aligned} \tag{33}$$

When $a=1$,

$$p_{d1} = \frac{\sqrt{2}}{4} + \frac{1}{\pi} - \frac{\sqrt{2}}{4\pi} \arctan \sqrt{8} = 0.53333 , \tag{34}$$

but for the case of $a \neq 1$, the analytical expression of $p_{d1}$ is very complicated as shown in Appendix.

Similarly, for the central single bond $p_{s1}$,

$$f_{G\ominus s1}(x) = f_{2k}(x)[a f_{2k+1}(x) f_{2k-1}(x)] , \tag{35}$$

then,

$$\begin{aligned} p_{s1} &= \frac{2a}{\pi} \int_0^\infty \frac{f_{2k}(x)[a f_{2k+1}(x) f_{2k-1}(x)]}{f_{2k}(x)[f_{2k+1}^2(x) + a^2 f_{2k-1}(x) f_{2k+1}(x) + f_{2k}^2(x)]} dx \\ &= \frac{2a}{\pi} \int_0^\infty \frac{\beta(x)/\alpha(x)}{\beta^2(x) + a^2 \beta(x)/\alpha(x) + 1} dx . \end{aligned} \tag{36}$$

The final result with $a=1$ is the same as that of $p_{d1}$,

$$p_{s1} = \frac{\sqrt{2}}{4} + \frac{1}{\pi} - \frac{\sqrt{2}}{4\pi} \arctan \sqrt{8} = 0.53333 . \tag{37}$$

The analytical expression for the case with $a \neq 1$ is given in Appendix.

It is interesting to see that the bond orders of the central double and single bonds are equal when $a=1$ for infinitely large $Y$ polymer. It means that as long as all the bond lengths are assumed equal, the bond orders of the central single and double bonds of infinitely large $Y$ network tend to

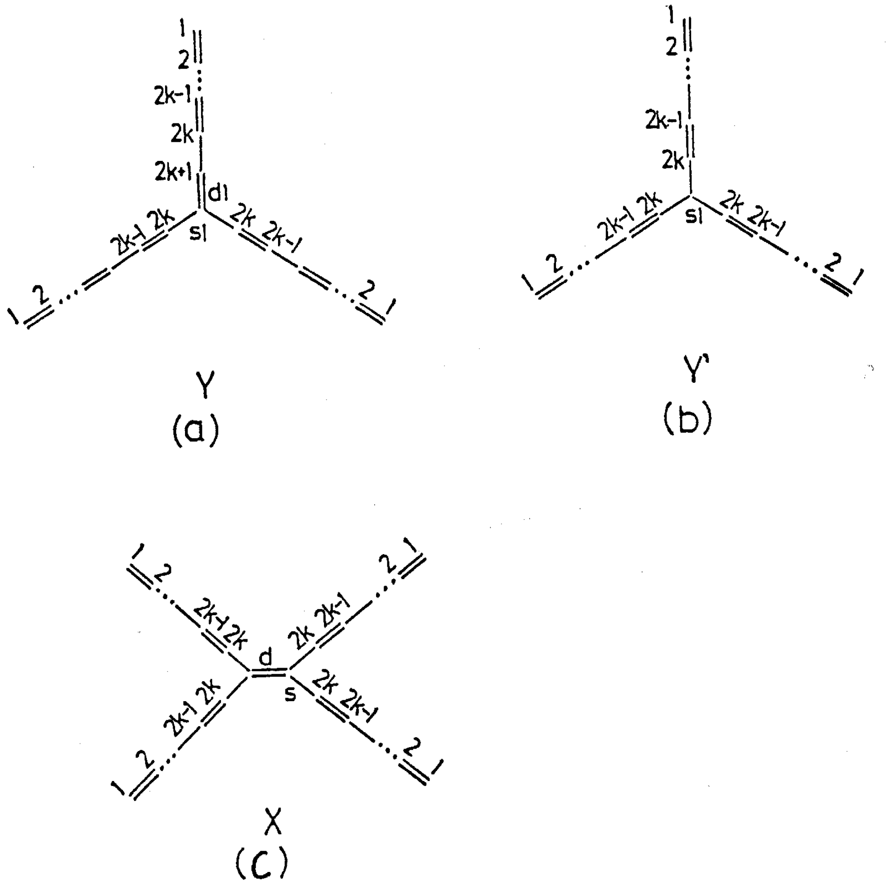

Chart 2.

be identical. This is just as the case with infinitely large polyacetylene [22].

The radical $Y'$ (see Chart 2(b)) looks analogous to network $Y$, which has three identical polyacetylenes having $2k+1$ carbon atoms. The three central bonds are all single bonds.

The bond order of the central bond of $Y'$ is similarly calculated as follows:

$$f_G(x)=f_{2k}^2(x)[f_{2k+1}(x)+2a^2f_{2k-1}(x)], \tag{38}$$

$$f_{G\ominus s1}(x)=af_{2k}^2(x)f_{2k-1}(x), \tag{39}$$

$$\begin{aligned} p_{s1}&=\frac{2}{\pi}\int_0^\infty \frac{af_{2k}(x)f_{2k-1}(x)}{f_{2k}(x)[f_{2k+1}(x)+2a^2f_{2k-1}(x)}dx \\ &=\frac{2a}{\pi}\int_0^\infty \frac{1}{\alpha(x)\beta(x)+2a^2}dx\,. \end{aligned} \tag{40}$$

The final results are:

for $a=1$: $p_s=\frac{\sqrt{2}}{4}+\frac{1}{\pi}-\frac{\sqrt{2}}{4\pi}\arctan\sqrt{8}=0.53333,$

and

for $a \neq 1$: $$p_s = \frac{4a^2-1}{8a\sqrt{3a^2+3/2}} + \frac{1}{\pi a}E(a) + \frac{(1-a)(4a+1)}{\pi a(2a+1)^2}K(a) - \frac{(2a-1)^2(1-a)^2}{6\pi a(1+a)(2a^2+1)}\Pi\left(\frac{(2a+1)^2}{6a^2+3}, \frac{2\sqrt{a}}{1+a}\right), \tag{41}$$

where $\Pi$ is the complete elliptic integral of the third kind,

$$\Pi(c, k) = \int_0^{\pi/2} \frac{d\theta}{(1+c\sin^2\theta)\sqrt{1-k^2\sin^2\theta}}. \tag{42}$$

In Fig. 2, the curves of the $a$-dependencies of $p_d$, $p_s$ for $Y$, and of $p_s$ for $Y'$ are shown.

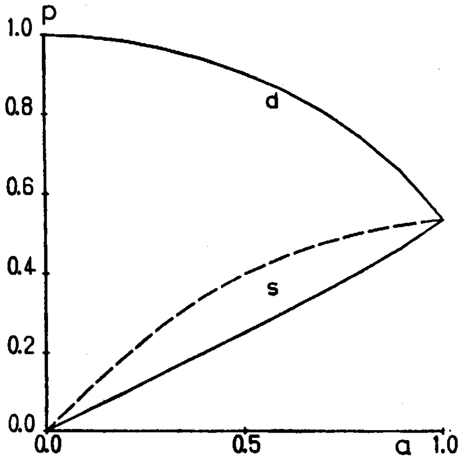

Fig. 2. The curves of the bond orders of the central bonds as a function of $a$. The ——— lines are those of polymer Y. The — — — line is that of Y′.

The analytical expressions of bond orders for infinitely large polyenes cannot always be obtained. For example, by extending the four linear branches at both ends of ethylene, we get the polyene skeleton $X$ as shown in Chart 2(c). The $p_d$, $p_s$ of $X$ are expressed as

$$p_d = \frac{2}{\pi}\int_0^{\infty} \frac{f_{G\ominus d}(x)}{f_G(x)}dx = \frac{2}{\pi}\int_0^{\infty} \frac{1}{[\beta(x)+a^2/\alpha(x)]^2+1}dx, \tag{43}$$

$$p_s = \frac{2}{\pi}\int_0^{\infty} \frac{f_{G\ominus s}(x)}{f_G(x)}dx = \frac{2}{\pi}\int_0^{\infty} \frac{a[\beta(x)\alpha(x)+a^2]}{[\beta(x)\alpha(x)+a^2]^2+\alpha^2(x)}dx. \tag{44}$$

The integrands of Eqs. (43) and (44) are so complicated that we cannot obtain the analytical expressions of the $p_d$ and $p_s$ for $X$. We draw the numerical solutions against $a$ as in Fig. 3. It can be seen from it that when $a$ is larger than 0.947 for $X$, the bond order of the central double bond is smaller than that of the single bond, so it can be said that for polymer $X$, bond alternation inevitably occurs.

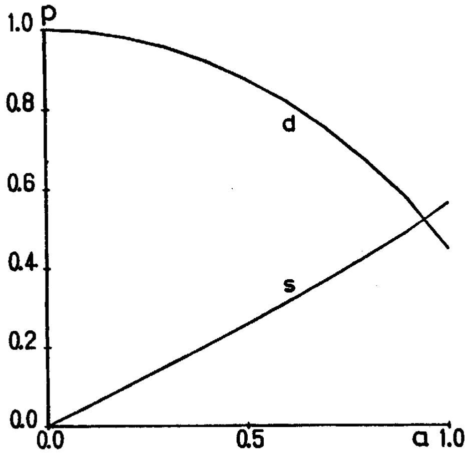

Fig. 3. The curves of the bond orders of the central bonds as a function of bond alternation parameter $a$ for polymer X.

## IV. Calculation of Infinitely Large Periodic Networks

Infinitely large one-dimensional periodic networks can be considered as cyclic polymers, as their physical properties are independent of the boundary conditions [27, 28]. For example, infinitely large polyacetylene can be constructed from the ethylene units as shown in Chart 3. Its characteristic polynomial is expressed as

$$P_G(x)=\Delta_G(x)=\prod_{k=1}^{N}\Delta_k(x)\,, \tag{45}$$

where $\Delta_k(x)$, the $k$-th factor of the characteristic polynomial, is

$$\Delta_k(x)=\begin{vmatrix} -x & 1+ac^k \\ 1+ac^{*k} & -x \end{vmatrix}=x^2-(1+2a\cos k\theta+a^2)\,, \tag{46}$$

with $c=\exp(i\theta)$ and $c^*=\exp(-i\theta)$, $(\theta=2\pi/N)$. Note that for large $N$, the argument $k\theta$ can be deemed as a continuously changing variable in the range of $0\leqq k\theta\leqq 2\pi$.

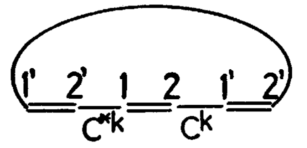

Chart 3.

Then, the bond order can be obtained from the following double integration involving $k$ vectors,

$$p_{rs}=(-1)^{r+s+1}\frac{1}{2\pi^2}\int_0^{2\pi}\int_{-\infty}^{\infty}\frac{\Delta_{k,rs}(iy)}{\Delta_k(iy)}dydk\theta\,, \tag{47}$$

where $\Delta_{k,rs}(x)$ is the subdeterminant obtained by deleting the $r$-th row and $s$-th column from $\Delta_k(x)$.

For example, in order to calculate the bond order $p_d$ of the central double bond for infinitely large polyacetylene, we get

$$\Delta_{k,d}(x) = -(1 + a \cos k\theta)\,, \tag{48}$$

by taking the average of the two cofactors $(r, s)$ and $(s, r)$ of $\Delta_k(x)$. Thus, according to Eq. (47), we can derive $p_d$ as,

$$p_d = \frac{2}{\pi^2}\int_0^\pi\int_0^\infty \frac{\Delta_{k,d}(ix)}{\Delta_k(ix)}dxdk\theta = \frac{2}{\pi^2}\int_0^\pi\int_0^\infty \frac{1 + a\cos k\theta}{x^2 + (1 + a^2 + 2a\cos k\theta)}dxdk\theta\,. \tag{49}$$

Finally, we get the known result,

$$p_d = \frac{2}{\pi}E(a)\,. \tag{50}$$

Calculation of the single bond can be performed just by interchanging the double and single bonds along the chain. Namely, we only need to change the $1+ac^k$ and $1+ac^{*k}$ in the off-diagonal element in $\Delta_k(x)$ into $a+c^k$ and $a+c^{*k}$, respectively. Thus we have,

$$\Delta_{k,s}(x) = -(a + \cos k\theta)\,, \tag{51}$$

and the bond order $p_s$ is obtained as

$$\begin{aligned} p_s &= \frac{2}{\pi^2}\int_0^\pi\int_0^\infty \frac{\Delta_{k,s}(ix)}{\Delta_k(ix)}dxdk\theta = \frac{2}{\pi^2}\int_0^\pi\int_0^\infty \frac{a + \cos k\theta}{x^2 + (1 + a^2 + 2a\cos k\theta)}dxdk\theta \\ &= \frac{2}{\pi a}[E(a) - (1 - a^2)K(a)]\,. \end{aligned} \tag{52}$$

The zeroes of $P_G(x)$ for infinitely large polyacetylene can easily be obtained from (46) as

$$x = \pm\sqrt{1 + 2a\cos k\theta + a^2}\,. \tag{53}$$

Then the total $\pi$-electronic energy is derived as

$$E_\pi = 2\sum_{k=1}^{N}\sqrt{1 + 2a\cos k\theta + a^2}\,, \tag{54}$$

For large $N$, the sum can be converted into an integral as

$$E_\pi = 2\frac{N}{\pi}\int_0^\pi \sqrt{1 + 2a\cos k\theta + a^2}\,dk\theta\,. \tag{55}$$

Since one unit has two electrons, the energy per $\pi$-electron is obtained as

$$\bar{\varepsilon}_\pi=\frac{E_\pi}{2N}=\frac{1}{\pi}\int_0^\pi\sqrt{1+2a\cos k\theta+a^2}\,dk\theta$$
$$=\frac{2}{\pi}[2E(a)-(1-a^2)K(a)]\,. \qquad (56)$$

It is obvious that, by using the cyclic model, the calculations are very simple and effective for infinitely large chains. In Ref. [23], we have shown the calculations by using this method for several periodic branched polyenes, and discussed the effects of branching on the bond alternation and electronic structure of polyacetylene.

Not only for the polyacetylene-like networks, but also for infinitely large periodic one-dimensional polycyclic aromatics, this method is found to be effective. In the following, we calculate the $\pi$-electronic energy and bond orders for the infinitely large polyacene and polyphenanthrene, with various modes of bond alternation, as shown in Fig. 4.

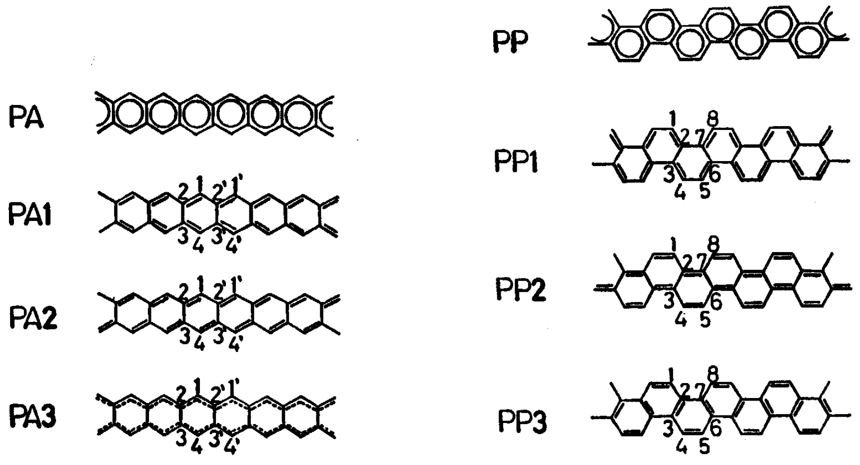

(a) (b)

Fig. 4. The structual isomers of polyacene (a) and polyphenanthrene (b).

Infinitely large polyacene can be considered to be constructed from butadiene units as shown in Fig. 5(a). Then the $k$-th factor of the characteristic polynomial with the bond alternation scheme of PA1 is

$$\Delta_k(x)=\begin{vmatrix} -x & 1+ac^k & 0 & 0 \\ 1+ac^{*k} & -x & a & 0 \\ 0 & a & -x & 1+ac^{*k} \\ 0 & 0 & 1+ac^k & -x \end{vmatrix}$$
$$=x^4-(3a^2+4a\cos k\theta+2)x^2+(a^2+2a\cos k\theta+1)^2\,, \qquad (57)$$

The subdeterminant $\Delta_{k,rs}(x)$ for bond 1, 2 is

$$\Delta_{k,12}(x)=-(1+a\cos k\theta)[x^2-(1+a^2+2a\cos k\theta)]\,. \tag{58}$$

Thus, according to Eq. (47), we can derive $p_{12}$ as follows,

$$\begin{aligned}
p_{12}&=\frac{2}{\pi^2}\int_0^\pi\int_0^\infty\frac{\Delta_{k,12}(ix)}{\Delta_k(ix)}dxdk\theta\\
&=\frac{2}{\pi^2}\int_0^\pi\int_0^\infty\frac{(1+a\cos k\theta)[x^2+(1+a^2+2a\cos k\theta)]}{x^4+(3a^2+4a\cos k\theta+2)x^2+(a^2+2a\cos k\theta+1)^2}dxdk\theta\\
&=\frac{2}{\pi^2}\int_0^\pi(1+a\cos k\theta)\int_0^\infty\frac{\{x^2+e\}}{\{x^2+g\}\{x^2+f\}}dxdk\theta\\
&=\frac{1}{\pi}\int_0^\pi(1+a\cos k\theta)\left[\left(\frac{e-g}{f-g}\right)\frac{1}{\sqrt{g}}+\left(\frac{f-e}{f-g}\right)\frac{1}{\sqrt{f}}\right]dk\theta\,,
\end{aligned} \tag{59}$$

where

$$g=\left[\frac{\sqrt{5a^2+8a\cos k\theta+4}+a}{2}\right]^2,\quad f=\left[\frac{\sqrt{5a^2+8a\cos k\theta+4}-a}{2}\right]^2,$$

and $e=(1+a^2+2a\cos k\theta)$.
Finally, we get the result as

$$\begin{aligned}
p_{12}&=\frac{1}{\pi}\int_0^\pi\frac{2(1+a\cos k\theta)}{\sqrt{5a^2+4+8a\cos k\theta}}dk\theta\\
&=\frac{4-5a^2}{2\pi\sqrt{5a^2+8a+4}}K\left(\sqrt{\frac{16a}{5a^2+8a+4}}\right)\\
&\qquad+\frac{\sqrt{5a^2+8a+4}}{2\pi}E\left(\sqrt{\frac{16a}{5a^2+8a+4}}\right),
\end{aligned} \tag{60}$$

Similarly, for bonds 2,3, 1,4 and 1′,2,

$$\Delta_{k,23}(x)=-ax^2, \tag{61}$$

$$\Delta_{k,14}(x)=-a(1+a^2+2a\cos k\theta)\,, \tag{62}$$

and

$$\Delta_{k,1'2}(x)=-(a+\cos k\theta)[x^2-(1+a^2+2a\cos k\theta)]\,. \tag{63}$$

Then, we get the noticeable results,

$$p_{23}=\frac{2a}{\pi\sqrt{5a^2+8a+4}}K\left(\sqrt{\frac{16a}{5a^2+8a+4}}\right)=-p_{14}\,. \tag{64}$$

$$\begin{aligned}
p_{1'2}&=\frac{3a^2-4}{2a\pi\sqrt{5a^2+8a+4}}K\left(\sqrt{\frac{16a}{5a^2+8a+4}}\right.\\
&\qquad+\frac{\sqrt{5a^2+8a+4}}{2a\pi}E\left(\sqrt{\frac{16a}{5a^2+8a+4}}\right).
\end{aligned} \tag{65}$$

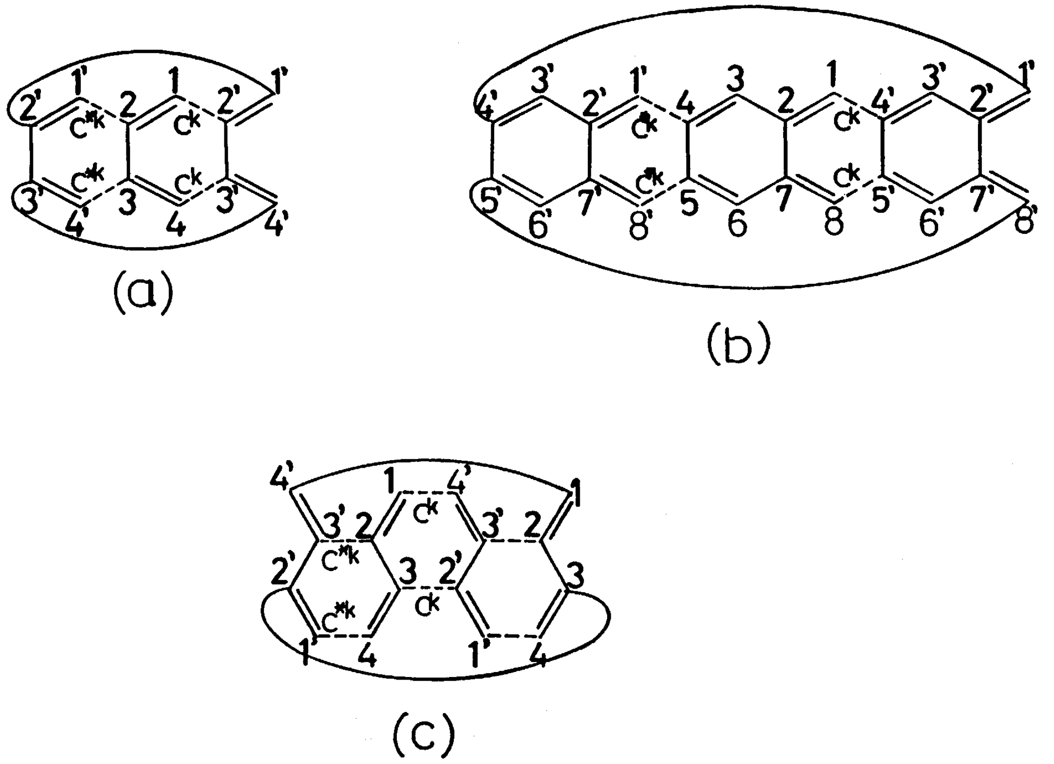

Fig. 5.

As will be known from Section IV, apart from the para bond 1,4, the bond order of the para bond $p_{2'3}$ is also necessary for calculating the benzene character of polyacene. However, since bond 2′,3 is not a bond in one butadiene unit, its bond order cannot be obtained by the present topological figure. We must expand the unit to be orthoquinodimethane, as shown in Fig. 5(b). Then the bond 2′,3 corresponds to the bond 4,7 in Fig. 5(b). The $k$-th factor of the characteristic polynomial, $\Delta_k(x)$, and the subdeterminant $\Delta_{k,47}(x)$ are obtained as

$$\Delta_k(x)=\begin{vmatrix} -x & 1 & 0 & ac^k & 0 & 0 & 0 & 0 \\ 1 & -x & a & 0 & 0 & 0 & a & 0 \\ 0 & a & -x & 1 & 0 & 0 & 0 & 0 \\ ac^{*k} & 0 & 1 & -x & a & 0 & 0 & 0 \\ 0 & 0 & 0 & a & -x & 1 & 0 & ac^{*k} \\ 0 & 0 & 0 & 0 & 1 & -x & a & 0 \\ 0 & a & 0 & 0 & 0 & a & -x & 1 \\ 0 & 0 & 0 & 0 & ac^k & 0 & 1 & -x \end{vmatrix}$$

$$\begin{aligned}&=x^8-2(3a^2+2)x^6+(11a^4+12a^2+6-4a^2\cos k\theta)x^4\\&\quad-2(3a^6+6a^4+3a^2+2-2a^4\cos k\theta-4a^2\cos k\theta)x^2\\&\quad+(a^4+1)^2+4a^4\cos^2 k\theta-4a^2(a^4+1)\cos k\theta\,,\end{aligned} \tag{66}$$

and

$$\Delta_{k,47}(x) = -2x^2a(x^2-a^2-1)(\cos k\theta+1)\,. \tag{67}$$

Then the bond order $p_{2'3}$ of the bond 2′,3 in Fig. 5(a) is derived as

$$p_{2'3} = \frac{2}{\pi^2}\int_0^\infty\int_0^\pi \frac{\Delta_{k,47}(ix)}{\Delta_k(ix)}\,dk\theta dx\,. \tag{68}$$

However, the analytical expression of (68) cannot be obtained. Its numerical results are plotted in Fig. 6, while the bond orders, $p_{12}$, $p_{23}$, $p_{14}$ and $p_{1'2}$, as a function of bond alternation parameter $a$, are also plotted.

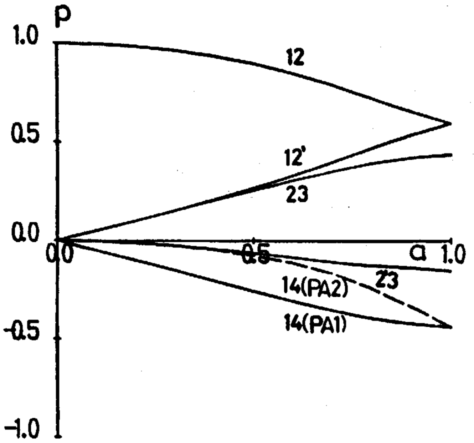

Fig. 6. The curves of the bond orders for PA1 and PA2 as a function of bond alternation parameter $a$. All the bond orders are identical for PA1 and PA2, except $p_{14}$.

Since the zeroes of $P_G(x)$ for PA1 are derived from Eq. (57) as

$$x = \pm\frac{1}{2}(a\pm\sqrt{5a^2+8a\cos k\theta+4})\,, \tag{69}$$

and one unit has $4\pi$-electrons, the energy per $\pi$-electron for PA1 is given by

$$\bar{\varepsilon}_\pi = \lim_{N\to\infty}\frac{E_\pi}{4N} = \frac{\sqrt{5a^2+8a+4}}{\pi}E\left(\sqrt{\frac{16a}{5a^2+8a+4}}\right). \tag{70}$$

It should be noted that, the relation between the bond orders and the $\pi$-electronic energy is obtained to be

$$\bar{\varepsilon}_\pi = \frac{1}{2}(2p_{12}+2ap_{1'2}+ap_{23})\,, \tag{71}$$

as expected from the scheme of the tight-binding approximation.

For PA2 and PA3, the processes of deriving the $\pi$-electronic energy and bond orders are the same as those applied to PA1, except that the factors of the characteristic polynomials of them are different from that of PA1, since they have different bond alternation patterns. The analytical expressions for PA1, PA2 and PA3 are given in Table I, while the bond orders $p_{12}$, $p_{23}$, $p_{14}$, and $p_{2'3}$ for PA3 are plotted in Fig. 7. Although the bond orders and the energy per $\pi$-electron of PA2 are all identical with those of PA1, the $p_{14}$ for PA2 is much more complicated than that of PA1.

Table I. The analytical expressions of bond orders $p_{12}$, $p_{23}$, $p_{1'2}$, $p_{14}$ and energy per $\pi$-electron $\bar{\varepsilon}_\pi$

| | |
|---|---|
| | $p_{12}$ |
| PA1 | $\frac{4-5a^2}{2\pi\sqrt{5a^2+8a+4}}K\left(\sqrt{\frac{16a}{5a^2+8a+4}}\right)+\frac{\sqrt{5a^2+8a+4}}{2\pi}E\left(\sqrt{\frac{16a}{5a^2+8a+4}}\right)$ |
| PA2 | $\frac{4-5a^2}{2\pi\sqrt{5a^2+8a+4}}K\left(\sqrt{\frac{16a}{5a^2+8a+4}}\right)+\frac{\sqrt{5a^2+8a+4}}{2\pi}E\left(\sqrt{\frac{16a}{5a^2+8a+4}}\right)$ |
| PA3 | $\frac{\sqrt{a^2+16}}{2\pi}\left[E\left(\frac{4}{\sqrt{a^2+16}}\right)-\frac{a^2}{a^2+16}K\left(\frac{4}{\sqrt{a^2+16}}\right)\right]$ |
| | $p_{23}$ |
| PA1 | $\frac{2a}{\pi\sqrt{5a^2+8a+4}}K\left(\sqrt{\frac{16a}{5a^2+8a+4}}\right)$ |
| PA2 | $\frac{2a}{\pi\sqrt{5a^2+8a+4}}K\left(\sqrt{\frac{16a}{5a^2+8a+4}}\right)$ |
| PA3 | $\frac{2a}{\pi\sqrt{a^2+16}}K\left(\frac{4}{\sqrt{a^2+16}}\right)$ |
| | $p_{1'2}$ |
| PA1 | $\frac{3a^2-4}{2a\pi\sqrt{5a^2+8a+4}}K\left(\sqrt{\frac{16a}{5a^2+8a+4}}\right)+\frac{\sqrt{5a^2+8a+4}}{2a\pi}E\left(\sqrt{\frac{16a}{5a^2+8a+4}}\right)$ |
| PA2 | $\frac{3a^2-4}{2a\pi\sqrt{5a^2+8a+4}}K\left(\sqrt{\frac{16a}{5a^2+8a+4}}\right)+\frac{\sqrt{5a^2+8a+4}}{2a\pi}E\left(\sqrt{\frac{16a}{5a^2+8a+4}}\right)$ |
| PA3 | $\frac{\sqrt{a^2+16}}{2\pi}\left[E\left(\frac{4}{\sqrt{a^2+16}}\right)-\frac{a^2}{a^2+16}K\left(\frac{4}{\sqrt{a^2+16}}\right)\right]$ |
| | $p_{14}$ |
| PA1 | $-\frac{2a}{\pi\sqrt{5a^2+8a+4}}K\left(\sqrt{\frac{16a}{5a^2+8a+4}}\right)$ |

Table I. Continued

| | |
|---|---|
| PA2 | $\frac{1+a^2}{\pi\sqrt{5a^2+8a+4}}K\left(\sqrt{\frac{16a}{5a^2+8a+4}}\right)-\frac{(1-a)^2}{\pi\sqrt{5a^2+8a+4}}\Pi\left(\frac{4a}{(1+a)^2},\sqrt{\frac{16a}{5a^2+8a+4}}\right)$ |
| PA3 | $-\frac{2a}{\pi\sqrt{a^2+16}}K\left(\frac{4}{\sqrt{a^2+16}}\right)$ |
| | $\bar{\varepsilon}_\pi$ |
| PA1 | $\frac{\sqrt{5a^2+8a+4}}{\pi}E\left(\sqrt{\frac{16a}{5a^2+8a+4}}\right)=\frac{1}{2}(2p_{12}+2ap_{1'2}+ap_{23})$ |
| PA2 | $\frac{\sqrt{5a^2+8a+4}}{\pi}E\left(\sqrt{\frac{16a}{5a^2+8a+4}}\right)=\frac{1}{2}(2p_{12}+2ap_{1'2}+ap_{23})$ |
| PA3 | $\frac{\sqrt{a^2+16}}{\pi}E\left(\frac{4}{\sqrt{a^2+16}}\right)=\frac{1}{2}(4p_{12}+ap_{23})$ |

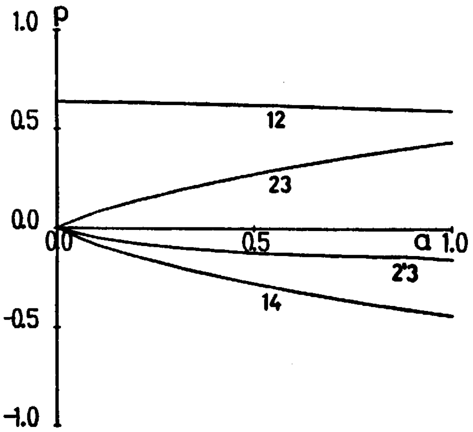

Fig. 7. The curves of the bond orders for PA3 as a function of bond alternation parameter $a$.

The curves of the energy per $\pi$-electron for PA1, PA2 and PA3 are shown in Fig. 8 as a function of bond alternation parameter $a$. PA3 is more stable than PA1 and PA2 in all the range of $0 \leq a \leq 1$. For an extreme case with $a=0$, PA1 and PA2 are decomposed into isolated ethylenes, with $\bar{\varepsilon}_\pi = 1.0(\beta)$. However, for the limiting case of PA3 with $a=0$, we get the result for polyacetylene with no bond alternation, having $\bar{\varepsilon}_\pi = 1.27324(\beta)$.

As shown in Fig. 5(c), polyphenanthrene can also be constructed from butadiene units in a different mode from polyacene. The characteristic polynomial for PP1 can be expressed as

$$P_G(x)=\Delta_G(x)=\prod_{k=1}^{N}\Delta_k(x)\,, \tag{72}$$

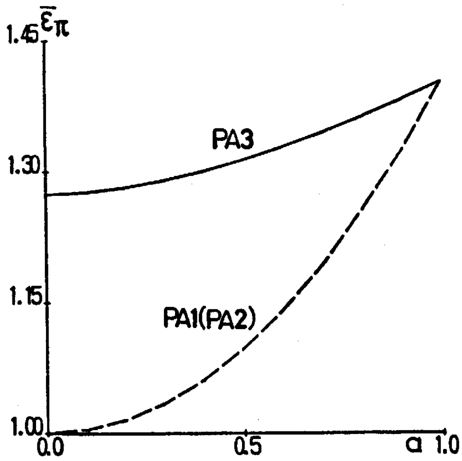

Fig. 8. The curves of the energies per $\pi$-electron as a function of parameter $a$ for PA1(PA2) and PA3.

where

$$\Delta_k(x)=\begin{vmatrix} -x & 1 & 0 & ac^k \\ 1 & -x & a(1+c^{*k}) & 0 \\ 0 & a(1+c^k) & -x & 1 \\ ac^{*k} & 0 & 1 & -x \end{vmatrix}$$

$$=x^4-x^2(3a^2+2+2a^2\cos k\theta)+[2a^4(1+\cos k\theta) -2a^2(2\cos^2 k\theta+\cos k\theta-1)+1]\,. \tag{73}$$

Similarly for PP2, the factor of the characteristic polynomial can be obtained according to the pattern of PP2 as in Fig. 4. Then, by the same process as polyacene, we obtained the analytical expressions of $\pi$-electronic energy and various bond orders for PP1 and PP2 as shown in Tables II and III, respectively. It is worthy of notice that, when $a=1$, Tables II and III coincide with each other.

The bond orders for PP1 and PP2 are plotted against parameter $a$ as shown in Figs. 9 and 10, respectively.

However, for PP3, we failed to obtain the analytical solutions of $\bar{\varepsilon}_\pi$ and the bond orders. Whether Eqs. (1) and (3) can be analytically integrated mostly depend on the fact that the denominator of the integrands can be factorized into a form like $(x^2+g)(x^2+f)$ with perfectly squared $g$ and $f$. For PP3, since $g$ and $f$ are not perfectly squared, its analytical results cannot be obtained. We plot the numerical values of the bond orders and $\bar{\varepsilon}_\pi$ in Figs. 11 and 12, respectively. $\bar{\varepsilon}_\pi$ of PP1 and PP2 are also shown in Fig. 12 by the dotted line and the dot-and-dash line respectively. Among the three isomers with different mode of bond alternation, PP3 is the most stable and PP1 the least stable.

Table II. The coefficients in front of $E(k_1)$, $K(k_1)$, $E(k_2)$ and $K(k_2)$ in the expressions of bond orders $p_{12}$, $p_{23}$, $p_{14}$, $p_{45}$, $p_{27}$, $p_{25}$ and $p_{36}$ for PP1. The expression of energy per $\pi$-electron $\bar{\varepsilon}_\pi$ is also shown.

| | | | | |
|---|---|---|---|---|
| $p_{12}$ | $A_1$ | $-B_1$ | $A_2$ | $-B_2$ |
| $p_{23}$ | $\frac{\sqrt{a^2+4}+a}{2}A_1$ | $-\left(\frac{\sqrt{a^2+4}+a}{2}\right)B_1$ | $-\left(\frac{\sqrt{a^2+4}-a}{2}\right)A_2$ | $\frac{\sqrt{a^2+4}-a}{2}B_2$ |
| $p_{14}$ | $\frac{\sqrt{a^2+4}-a}{2}A_1$ | $-\left(\frac{\sqrt{a^2+4}-a}{2}\right)B_1$ | $-\left(\frac{\sqrt{a^2+4}+a}{2}\right)A_2$ | $\frac{\sqrt{a^2+4}+a}{2}B_2$ |
| $p_{45}$ | $\frac{1}{a}A_1$ | $\frac{1}{a}B_1$ | $\frac{1}{a}A_2$ | $\frac{1}{a}B_2$ |
| $p_{27}$ | $\left(\frac{\sqrt{a^2+4}+a}{4a}\right)^2 A_1$ | $\left(\frac{\sqrt{a^2+4}+a}{4a}\right)^2 B_1$ | $\left(\frac{\sqrt{a^2+4}-a}{4a}\right)^2 A_2$ | $\left(\frac{\sqrt{a^2+4}-a}{4a}\right)^2 B_2$ |
| $p_{25}$ | $\frac{\sqrt{a^2+4}+a}{2a}A_1$ | $\frac{\sqrt{a^2+4}+a}{2a}B_1$ | $-\left(\frac{\sqrt{a^2+4}-a}{2a}\right)A_2$ | $-\left(\frac{\sqrt{a^2+4}-a}{2a}\right)B_2$ |
| $p_{36}$ | $\frac{\left[(\sqrt{a^2+4}+a)^2-8a^2\right]}{12a}A_1$ | $\frac{\left[(\sqrt{a^2+4}+a)^2+8a^2\right]}{12a}B_1$ | $\frac{\left[(\sqrt{a^2+4}-a)^2-8a^2\right]}{12a}A_2$ | $\frac{\left[(\sqrt{a^2+4}-a)^2+8a^2\right]}{12a}B_2$ |

$$\bar{\varepsilon}_\pi=\frac{1}{2\pi}\left[(3a+\sqrt{a^2+4})E(k_1)+(a+\sqrt{a^2+4})E(k_2)\right]-\frac{1}{2}(2p_{12}+ap_{23}+ap_{45}+ap_{27})$$

$$A_1=a\sqrt{a^2+4}+2-a^2 \qquad A_2=a\sqrt{a^2+4}+2+a^2$$

$$B_1=a\sqrt{a^2+4}-2-a^2 \qquad B_2=a\sqrt{a^2+4}-2+a^2$$

$$k_1=\frac{2\sqrt{2a(\sqrt{a^2+4}+a)}}{a\sqrt{a^2+4}+2+a^2} \qquad k_2=\frac{2\sqrt{2a(\sqrt{a^2+4}+a)}}{a\sqrt{a^2+4}+2+a^2}$$

Both in Figs. 9 and 10, there is a region where the relative values of bond orders are in contradiction with the bond alternation pattern. For example, for PP1, when $a$ is larger than 0.82, the bond order $p_{45}$ for a single bond is larger than $p_{12}$, for a double bond. For PP2, when $a$ is larger than 0.85, $p_{23}$, for a single bond is larger than that of the double bond $p_{27}$. Thus only when $a$ is smaller than 0.82 and 0.85 for PP1 and PP2, respectively, the relative values of the bond orders are consistent with their bond alternation patterns.

There is no crossing point in Fig. 11, and the relative values of bond orders are consistent with the bond alternation pattern in Fig. 4. We

Table III. The coefficients in front of $E(k_1)$, $K(k_1)$, $E(k_2)$ and $K(k_2)$ in the expressions of bond orders $p_{12}$, $p_{23}$, $p_{14}$, $p_{45}$, $p_{27}$, $p_{25}$ and $p_{36}$ for PP2. The expression of energy per π-electron $\bar{\varepsilon}_\pi$ is also shown.

| | | | | |
|---|---|---|---|---|
| $p_{12}$ | $\frac{1}{a}G_1$ | $\frac{1}{a}G_2$ | $\frac{1}{a}G_3$ | $\frac{1}{a}G_4$ |
| $p_{23}$ | $\frac{\sqrt{5}+1}{2a}G_1$ | $-\left(\frac{\sqrt{5}+1}{2a}\right)G_2$ | $-\left(\frac{\sqrt{5}-1}{2a}\right)G_3$ | $\frac{\sqrt{5}-1}{2a}G_4$ |
| $p_{14}$ | $\frac{\sqrt{5}-1}{2a}G_1$ | $-\left(\frac{\sqrt{5}-1}{2a}\right)G_2$ | $-\left(\frac{\sqrt{5}+1}{2a}\right)G_3$ | $\frac{\sqrt{5}+1}{2a}G_4$ |
| $p_{45}$ | $G_1$ | $G_2$ | $G_3$ | $G_4$ |
| $p_{27}$ | $\frac{3+\sqrt{5}}{2}G_1$ | $\frac{3+\sqrt{5}}{2}G_2$ | $\frac{3-\sqrt{5}}{2}G_3$ | $\frac{3-\sqrt{5}}{2}G_4$ |
| $p_{25}$ | $\frac{\sqrt{5}+1}{2}G_1$ | $\frac{\sqrt{5}+1}{2}G_2$ | $-\left(\frac{\sqrt{5}-1}{2}\right)G_3$ | $-\left(\frac{\sqrt{5}-1}{2}\right)G_4$ |
| $p_{36}$ | $\frac{(3+\sqrt{5})a^2-4}{6}G_1$ | $\frac{(3+\sqrt{5})a^2+4}{6}G_2$ | $\frac{(3-\sqrt{5})a^2-4}{6}G_3$ | $\frac{(3-\sqrt{5})a^2+4}{6}G_4$ |

$$\bar{\varepsilon}_\pi = \frac{5+\sqrt{5}}{2}G_1E(k_1) + \frac{5-\sqrt{5}}{2}G_3E(k_2) - \frac{1}{2}(2ap_{12} + ap_{23} + p_{45} + p_{27})$$

$$G_1 = \frac{2a+\sqrt{5}-1}{2\pi\sqrt{5}}, \quad G_2 = \frac{-2a+\sqrt{5}-1}{2\pi\sqrt{5}},$$

$$G_3 = \frac{2a+\sqrt{5}+1}{2\pi\sqrt{5}}, \quad G_4 = \frac{-2a+\sqrt{5}+1}{2\pi\sqrt{5}},$$

$$k_1 = \frac{2\sqrt{2a(\sqrt{5}+1)}}{(\sqrt{5}+1)a+2}, \quad k_2 = \frac{2\sqrt{2a(\sqrt{5}-1)}}{(\sqrt{5}-1)a+2}.$$

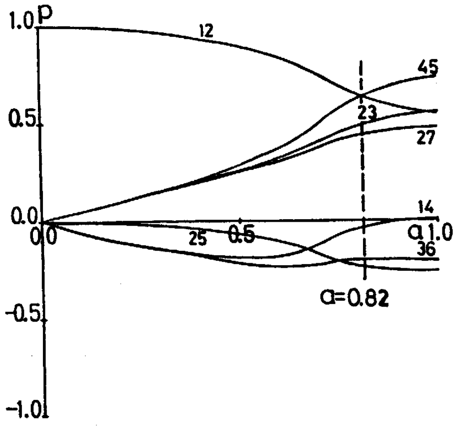

Fig. 9. The curves of the bond orders as a function of parameter *a* for PP1.

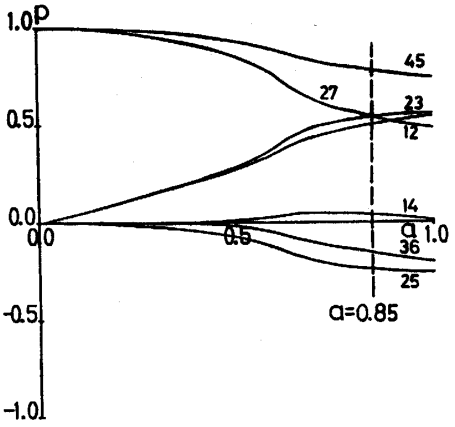

Fig. 10. The curves of the bond orders as a function of parameter *a* for PP2.

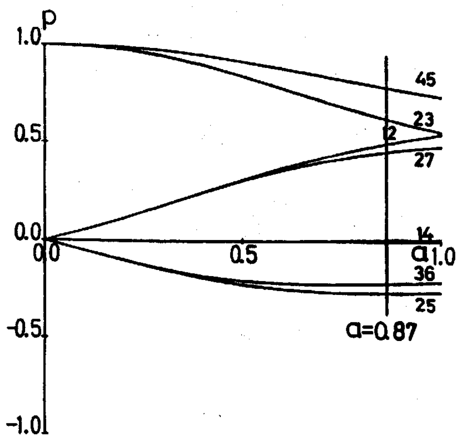

Fig. 11. The $a$-dependency of the bond orders of PP3. For the values at $a=0.87$, the bond orders agree quite well with those obtained by Tanaka et al., by using the so-called one-dimensional tight-binding SCF-CO method.

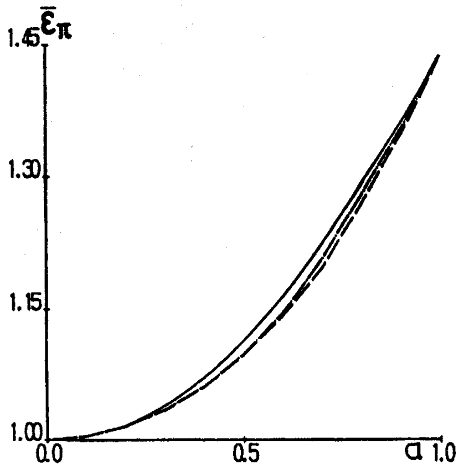

Fig. 12. The curves of the energies per $\pi$-electron as a function of parameter $a$. The dotted, dashed line with dots and solid lines are those for PP1, PP2 and PP3, respectively.

think PP3 is the most favorable isomer for polyphenanthrene with respect to bond orders.

In Ref. [29], Tanaka et al. have given the calculated results of bond orders of $p_{45}$, $p_{12}$, $p_{27}$, and $p_{23}$ as 0.785, 0.502, 0.463, and 0.615, respectively, by the one-dimensional tight-binding SCF-CO (crystal orbital) method. Those bond orders have no large difference from our results, 0.784, 0.499, 0.456, and 0.635, obtained with the parameter $a=0.87$ for PP3. Here, it is worthy of notice that when the bond alternation is properly considered in the HMO calculation, one can reproduce the results obtained by a more elaborate method.

## IV. MO-Benzene Character for Polycyclic Aromatics

For an alternant hydrocarbon, MO-benzene character was defined by Polansky et al. [30] by using the Coulson's bond orders as follows,

$$r_L=\frac{1}{2}+\frac{1}{18}\left(2\sum^{L} p_{\mathrm{ortho}}-\sum^{L} p_{\mathrm{para}}\right), \tag{74}$$

where $p_{\mathrm{ortho}}$ is the Coulson's bond order of a pair of adjacent atoms in a given benzene ring $L$, and $p_{\mathrm{para}}$ is that of a pair of para atoms.

In order to make the benzene character vary from 0 for three isolated double bonds to 1.0 for benzene, Aida et al. [31] defined the normalized MO-benzene character as

$$\bar{r}_L = 6r_L - 5$$
$$= \frac{1}{3}\left(2 \sum^{L} p_{\text{ortho}} - \sum^{L} p_{\text{para}}\right) - 2 . \tag{75}$$

For the polyacene isomers, we get the following expression easily,

$$\bar{r}_L = \frac{4}{3}(p_{12} + p_{23} + p_{12'}) - \frac{1}{3}(p_{14} + 2p_{2'3}) - 2 . \tag{76}$$

For PA1 and PA2, because only the bond order $p_{14}$ is different, the difference of their benzene characters can simply be expressed as

$$\Delta(\bar{r}_L) = -\frac{1}{3}\Delta(p_{14}) . \tag{77}$$

As the analytical expression of bond order $p_{2'3}$ cannot be obtained, we can only show the numerical results of $\bar{r}_L$ for the polyacene isomers as in Fig. 13. It is easily seen that PA3 has the largest benzene character as expected.

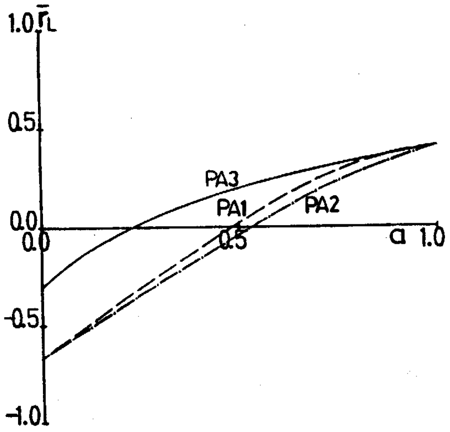

Fig. 13. The curves of the benzene characters against parameter *a* for PA1, PA2 and PA3, respectively.

For the polyphenanthrene isomers, $\bar{r}_L$ can be expressed as

$$\bar{r}_L = \frac{2}{3}(2p_{12} + 2p_{23} + p_{27} + p_{45}) - \frac{1}{3}(2p_{25} + p_{36}) - 2 . \tag{78}$$

We have obtained the analytical solutions of all the bond orders for polyphenanthrene PP1 and PP2. Thus by substituting the formulas of these bond orders into Eq. (78), the analytical expression of $\bar{r}_L$ for PP1 can be obtained as

$$\begin{aligned}\bar{r}_L=\frac{1}{18}\{&[(17a-6)\sqrt{a^2+4}+(21a^2+18a+22)]A_1E(k_1)\\&-[(7a+6)\sqrt{a^2+4}+(11a^2+30a-22)]B_1K(k_1)\\&-[(17a-6)\sqrt{a^2+4}-(21a^2+18a+22)]A_2E(k_2)\\&+[(7a+6)\sqrt{a^2+4}-(11a^2+30a-22)]B_2K(k_2)\}-2\,,\end{aligned}\tag{79}$$

and for PP2, $\bar{r}_L$ is expressed as

$$\begin{aligned}\bar{r}_L=&\frac{3+\sqrt{5}}{18a}\{[12+7(3-\sqrt{5})a-a^3]G_1E(k_1)\\&\qquad-[12-5(3-\sqrt{5})a+a^3]G_2K(k_1)\}\\&+\frac{3-\sqrt{5}}{18a}\{[12+7(3+\sqrt{5})a-a^3]G_3E(k_2)\\&\qquad-[12-5(3+\sqrt{5})a+a^3]G_4K(k_2)\}-2\,.\end{aligned}\tag{80}$$

For PP3, the numerical results of $\bar{r}_L$ are plotted in Fig. 14. The curves of $\bar{r}_L$ as a function of parameter $a$ for PP1 and PP2 are also plotted. It is seen that the component hexagon of PP3 has the largest benzene property in all the range of $0\leqq a\leqq 1$. The curve of PP3 has a maximum when $a$ is about 0.7.

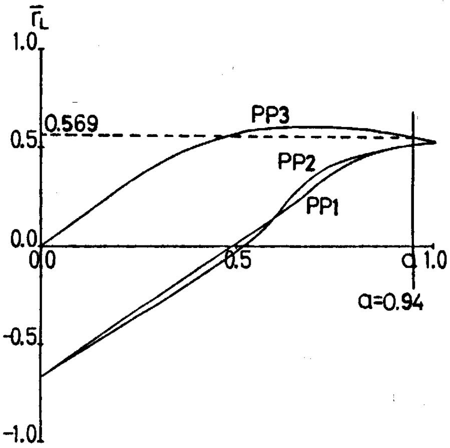

Fig. 14. The curves of the benzene characters against parameter $a$ for PP1, PP2 and PP3, respectively.

According to Ref. [31], in the PPP calculation, as the network of polyphenanthrene is large enough, (having about 25 rings), the value of the benzene character $\bar{r}_L$ of the central ring converges to 0.56947. This value is found to correspond with our result of PP3 with $a=0.94$. However, for PP1 and PP2, in all the range of $0\leqq a\leqq 1$, $\bar{r}_L$ of HMO calculation gets never larger than 0.52630, and there is no $a$ value compatible with that PPP. In this respect, PP3 is also considered to be the best candidate among the bond alternation isomers.

## V. Concluding Remarks

(1) The two approaches proposed by us are shown to be very powerful for calculating $\bar{\varepsilon}_\pi$ and bond orders of infinitely large networks. Furthermore, we found that these methods can also be expanded to two-dimensional periodic networks, such as graphite, as will be discussed elsewhere.

(2) For infinitely large polyacene with bond alternation, the $\pi$-electronic structure of PA3 is found to be the most stable in the range of $0 \leqq a < 1$. For infinitely large polyphenanthrene with bond alternation, the $\pi$-electronic structure of PP3 is the most stable, and the most plausible one with respect to the bond orders and benzene character.

(3) It was shown that if the bond alternation is properly taken into consideration in the HMO calculation of large periodic $\pi$-electronic networks, we can get rather reliable results as compatible with more sophisticated methods, such as PPP and SCF-CO calculations.

**Acknowledgments:**

This work was supported by the Grant-in-Aid for Scientific Research from the Ministry of Education, Science and Culture, Japanese Government.

## Appendix

The analytical expression of the bond order of the central double bond for polyene $Y_G$ is

$$\text{for } a=1: \quad p_{d1}=\frac{\sqrt{2}}{4}+\frac{1}{\pi}-\frac{\sqrt{2}}{4\pi}\arctan\sqrt{8}=0.53333,$$

$$\text{for } a\neq 1: \quad p_{d1}=\frac{4-a^2}{4\sqrt{2}\sqrt{a^2+8}}+\frac{1}{\pi}E(a)+\frac{a^2+2a-4}{2\pi}K(a)$$

$$+\frac{1-a}{4\pi(1+a)\sqrt{a^2+8}}\left\{[a^2+3a+8-(a+3)\sqrt{a^2+8}]\Pi\left(\frac{a(8-a-3\sqrt{a^2+8}}{4(1+a)^2},\frac{2\sqrt{a}}{1+a}\right)\right.$$

$$\left.-[a^2+3a+8+(a+3)\sqrt{a^2+8}]\Pi\left(\frac{a(8-a+3\sqrt{a^2+8}}{4(1+a)^2},\frac{2\sqrt{a}}{1+a}\right)\right\}. \quad (81)$$

The analytical expression of the bond order $p_{s1}$ is

$$\text{for } a=1: \quad p_{s1}=\frac{\sqrt{2}}{4}+\frac{1}{\pi}-\frac{\sqrt{2}}{4\pi}\arctan\sqrt{8}=0.53333,$$

$$\text{for } a \neq 1: \quad p_{s1} = \frac{9\sqrt{2}\,a(a^2+2+a\sqrt{a^2+8})}{16(1-a^2)\sqrt{a^2+8}} + \frac{1}{\pi a}E(a) + \frac{15a^2-4a-8}{8a\pi}$$
$$+\frac{1-a}{2\pi(1+a)\sqrt{a^2+8}}\left\{(\sqrt{a^2+8}-3)\Pi\left(\frac{a(8-a+3\sqrt{a^2+8})}{4(1+a)^2}, \frac{2\sqrt{a}}{1+a}\right)\right.$$
$$\left.-(\sqrt{a^2+8}+3)\Pi\left(\frac{a(8-a-3\sqrt{a^2+8})}{4(1+a)^2}, \frac{2\sqrt{a}}{1+a}\right)\right\}. \quad (82)$$

## References

[1] J. E. Lennard-Jones: Proc. R. Soc. Ser. A, **158** (1937) 280.
[2] C. A. Coulson and G. R. Rushbrooke: Proc. R. Soc. Edin. Ser. A, **62** (1948) 336.
[3] C. A. Coulson: Proc. Phys. Soc. London, **60** (1948) 257.
[4] Y. Ooshika: J. Phys. Soc. Jpn., **12** (1957) 1246.
[5] L. Salem and H. C. Longuet-Higgins: Proc. R. Soc. Ser., **A255** (1960) 435.
[6] S. Yomosa: J. Phys. Soc. Jpn., **19** (1964) 1718.
[7] I. Gutman and N. Trinajstić: Z. Naturforsch, Teil A, **29** (1974) 1238.
[8] O. E. Polansky and N. Tyutyulkov: MATCH, **3** (1977) 149.
[9] M. V. Kaulgud and V. H. Chitgopkar: J. Chem. Soc. Faraday Trans, **2**, 73 (1977) 1385.
[10] J. K. Burdett and S. Lee: J. Am. Chem. Soc., **107** (1985) 3063.
[11] U. Norinder and O. Wennerström: Tetrahedron, **41** (1985) 713.
[12] I. Gutman, A. V. Teodorović and Lj. Nedeljković: Theoret. Chim. Acta (Beri.), **65** (1984) 23.
[13] Tomislav P. Zivković: Theor. Chim. Acta, **73** (1988) 207.
[14] J. Cioslowski and O. E. Polansky: Theor. Chim. Acta, **74** (1988) 55.
[15] L. J. Schaad, B. A. Hess, Jr., J. B. Nation, N. Trinajstić and I. Gutman: Croat. Chem. Acta, **52** (1979) 233.
[16] E. Heilbronner: Helv. Chim. Acta, **37** (1954) 921.
[17] T. X. Lü, Y. S. Jiang and A. Q. Tang: Acta Phys. Chim. Sin., **1** (1985) 556.
[18] A. Graovac, O. E. Polansky and N. N. Tyutyulkov: Croat. Chem. Acta, **56** (1983) 325.
[19] M. Kertesz, Y. S. Lee and J. J. P. Stewart: Int. J. Quantum Chem., **35** (1989) 305.
[20] N. Tyutyulkov, P. Schuster and O. Polansky: Theor. Chim. Acta (Berl.), **291** (1983) 63.
[21] T. Kanazawa and H. Hosoya: Int. J. Quant. Chem., **15** (1979) 243.
[22] H. Hosoya and A. Tsuchiya: J. Molecular Structure (Theochem), **185** (1989) 123.
[23] Y.-D. Gao and H. Hosoya: J. Molecular Structure (Theochem), **206** (1990) 153.
[24) Y.-D. Gao and H. Hosoya: Theor. Chim. Acta, submitted.
[25] C. A. Coulson and H. C. Longuet-Higgins: Proc. Roy. Soc. London, **A191** (1947) 39.
[26] M. Abramowitz and I. A. Stegun (Eds.): Handbook of Mathematical Funtcions, Natl. Bur. Stand., Washington, D. C., 1964.
[27] W. Ledermann: Proc. R. Soc., A182 (1944) 362.
[28] H. Hosoya, M. Aida, R. Kumagai and K. Watanabe: J. Comput. Chem., 8 (1987) 358.
[29] K. Tanaka, K. Ohzeki, S. Nankai, T. Yamabe and H. Shirakawa: J. Phys. Chem. Soilds, **44** (1983) 1069.
[30] O. E. Polansky and G. Derflinger: Int. J. Quantum Chem., **1** (1967) 379.
[31] M. Aida and H. Hosoya: Tetrehedron, **36** (1980) 1317.